Article

Hypoxia-Targeting Copper Bis(selenosemicarbazone) Complexes: Comparison with Their Sulfur Analogues

Thomas C. Castle, Richard I. Maurer, Frank E. Sowrey, Michael J. Went, Christopher A. Reynolds, Eric J. L. McInnes, and Philip J. Blower

J. Am. Chem. Soc., **2003**, 125 (33), 10040-10049• DOI: 10.1021/ja035737d • Publication Date (Web): 26 July 2003

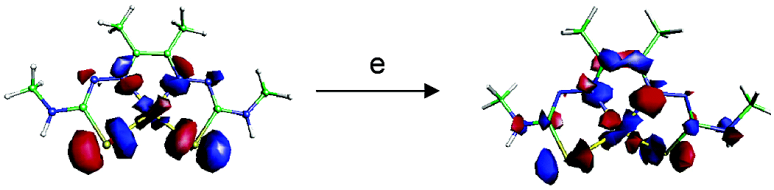

More About This Article

Additional resources and features associated with this article are available within the HTML version:

- Supporting Information
- Links to the 5 articles that cite this article, as of the time of this article download
- Access to high resolution figures
- Links to articles and content related to this article
- Copyright permission to reproduce figures and/or text from this article

View the Full Text HTML

J|A|C|S
ARTICLES
Published on Web 07/26/2003

Hypoxia-Targeting Copper Bis(selenosemicarbazone) Complexes: Comparison with Their Sulfur Analogues

Thomas C. Castle,[†] Richard I. Maurer,[‡] Frank E. Sowrey,[†] Michael J. Went,[†] Christopher A. Reynolds,[‡] Eric J. L. McInnes,[§] and Philip J. Blower*,[⊥]

Contribution from the School of Physical Sciences, University of Kent, Canterbury CT2 7NR, United Kingdom, Department of Biological Sciences, University of Essex, Wivenhoe Park, Colchester, United Kingdom, EPSRC Multi-frequency EPR Service, Dept of Chemistry, The University of Manchester, Manchester M13 9PL, United Kingdom, and Research School of Biosciences, University of Kent, Canterbury CT2 7NJ, United Kingdom

Received April 22, 2003; E-mail: P.J.Blower@kent.ac.uk

Abstract: The first copper bis(selenosemicarbazone) complexes have been synthesized, using the ligands glyoxal bis(selenosemicarbazone), pyruvaldehyde bis(selenosemicarbazone), and 2,3-butanedione bis(selenosemicarbazone). Their spectroscopic properties indicate that they are structurally analogous to their well-known square-planar sulfur-containing counterparts, the copper bis(thiosemicarbazone) complexes. Spectroscopic comparison of the sulfur- and selenium-containing complexes provides insight into their electronic structure. The effects on spectroscopic and redox properties of replacing sulfur with selenium, and of successive addition of methyl groups to the ligand backbone, are rationalized in terms of their electronic structure using spin-unrestricted density functional calculations. These suggest that, like the sulfur analogues, the complexes have a very low-lying empty ligand-based π-orbital immediately above the LUMO, while the LUMO itself has $d_{x^2-y^2}$ character (i.e., is the spin partner of the HOMO). Replacement of S by Se shifts the oxidation potentials much more than the reduction potentials, whereas alkylation of the ligand backbone shifts the reduction potentials more than the oxidation potentials. This suggests that oxidation and reduction involve spatially different orbitals, with the additional electron in the reduced species occupying the ligand-based π-orbital rather than $d_{x^2-y^2}$. Density functional calculations on the putative singlet Cu(I)-reduced species suggest that this ligand π-character could be brought about by distortion away from planarity during reduction, allowing the low-lying ligand π-LUMO to mix into the $d_{x^2-y^2}$-based HOMO. The analogy in the structure and reduction behavior between the sulfur- and selenium-containing complexes suggests that labeled with positron emitting isotopes of copper (Cu-60, Cu-62, Cu-64), the complexes warrant biological evaluation as radiopharmaceuticals for imaging of tissue perfusion and hypoxia.

Introduction

Copper complexes with bis(thiosemicarbazone) ligands, first synthesized in the 1950s,[1−3] have anti-cancer chemotherapeutic[4] and superoxide dismutase-like activity,[5] and in radiolabeled form have been used as positron emission-imaging agents for blood perfusion[6] and most recently, tissue hypoxia.[7−9] The prototype hypoxia imaging complex is CuATSM (**3d**, Scheme 1).[10−22] Much of this biological activity involves processes of reduction, reoxidation, and dissociation. For example, the hypoxia-selectivity of CuATSM[7,9] is brought about by the addition of a single methyl group to the ligand backbone of the nonselective complex CuPTSM ($PTSMH_2$ = pyruvaldehyde bis(thiosemicarbazone)), causing both a shift in its Cu(II/I) redox potential of approximately −80 mV and a slower rate of acid-catalyzed dissociation following reduction.[23]

[†] School of Physical Sciences, University of Kent.
[‡] University of Essex.
[§] University of Manchester.
[⊥] Research School of Biosciences, University of Kent.

(1) Bahr, G. *Z. Anorg. Allg. Chem.* **1952**, *268*, 351−363.
(2) Bahr, G. *Z. Anorg. Allg. Chem.* **1953**, *273*, 325−332.
(3) Bahr, G.; Schleitzer, E. *Z. Anorg. Allg. Chem.* **1955**, *278*, 136−154.
(4) Petering, D. H. In *Metal Ions in Biological Systems*; Sigel, H., Ed.; Marcel Dekker: New York, 1980; Vol. 11, pp 197−229.
(5) Wada, A.; Fujibayashi, Y.; Yokoyama, A. *Arch. Biochem. Biophys.* **1994**, *310*, 1−5.
(6) Mathias, C. J.; Welch, M. J.; Raichle, M. E.; Mintun, M. A.; Lich, L. L.; McGuire, A. H.; Zinn, K. R.; John, E.; Green, M. A. *J. Nucl. Med.* **1990**, *31*, 351−359.
(7) Dearling, J. L. J.; Lewis, J. S.; McCarthy, D. W.; Welch, M. J.; Blower, P. J. *Chem. Commun.* **1998**, 2531−2532.
(8) Dearling, J. L. J.; Lewis, J. S.; Mullen, G. E. D.; Rae, M. T.; Zweit, J.; Blower, P. J. *Eur. J. Nucl. Med.* **1998**, *25*, 788−792.
(9) Dearling, J. L. J.; Lewis, J. S.; Mullen, G. E. D.; Welch, M. J.; Blower, P. J. *J. Biol. Inorg. Chem.* **2002**, *7*, 249−259.
(10) Chao, K. S. C.; Bosch, W. R.; Mutic, S.; Lewis, J. S.; Dehdashti, F.; Mintun, M. A.; Dempsey, J. F.; Perez, C. A.; Purdy, J. A.; Welch, M. J. *Int. J. Radiat. Oncol., Biol., Phys.* **2001**, *49*, 1171−1182.
(11) Fujibayashi, Y.; Cutler, C. S.; Anderson, C. J.; McCarthy, D. W.; Jones, L. A.; Sharp, T.; Yonekura, Y.; Welch, M. J. *Nucl. Med. Biol.* **1999**, *26*, 117−121.
(12) Fujibayashi, Y.; Taniuchi, H.; Yonekura, Y.; Ohtani, H.; Konishi, J.; Yokoyama, A. *J. Nucl. Med.* **1997**, *38*, 1155−1160.
(13) Fujibayashi, Y.; Yoshimi, E.; Waki, A.; Takahashi, N.; Yonekura, Y. *J. Nucl. Med.* **1998**, *38*, 503P.
(14) Lewis, J. S.; Laforest, R.; Buettner, T. L.; Song, S. K.; Fujibayashi, Y.; Connett, J. M.; Welch, M. J. *Proc. Natl. Acad. Sci. U.S.A.* **2001**, *98*, 1206−1211.
(15) Lewis, J. S.; McCarthy, D. W.; McCarthy, T. J.; Fujibayashi, Y.; Welch, M. J. *J. Nucl. Med.* **1999**, *40*, 177−183.
(16) Lewis, J. S.; Sharp, T. L.; Laforest, R.; Fujibayashi, Y.; Welch, M. J. *J. Nucl. Med.* **2001**, *42*, 655−661.

10.1021/ja035737d CCC: $25.00

Scheme 1. Synthesis of Bis(selenosemicarbazone) Ligands and Naming of Complexes

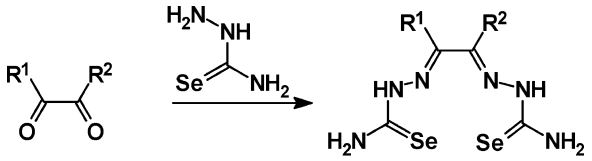

1a $R^1 = R^2 = H$
1b $R^1 = H$, $R^2 = CH_3$
1c $R^1 = R^2 = CH_3$

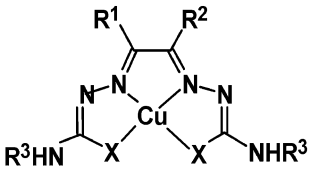

		R^1	R^2	R^3	X
2a	CuGSS	H	H	H	Se
2b	CuPSS	H	CH_3	H	Se
2c	CuASS	CH_3	CH_3	H	Se
2d	CuASSM	CH_3	CH_3	CH_3	Se
3a	CuGTS	H	H	H	S
3b	CuPTS	H	CH_3	H	S
3c	CuATS	CH_3	CH_3	H	S
3d	CuATSM	CH_3	CH_3	CH_3	S

It has been suggested that these marked effects of backbone alkylation are mediated by frontier orbitals that differ little in energy but greatly in spatial properties.[23] Thus, subtle energy shifts have profound chemical consequences because they alter the order, and hence the occupancy, of frontier orbitals. Using backbone alkylation in this way allows maintenance of hypoxia selectivity while controlling other pharmacokinetic properties through other structural modifications. For example, CuATSM (**3d**) and CuATS (**3c**) are both hypoxia-selective at the cellular level, but the former is able to cross the blood−brain barrier while the latter is not.[24]

We are now seeking to widen the range of properties further, both by varying the alkylation pattern of the ligand and by altering the donor atoms. Here we report the first selenium-containing analogues of these complexes. Monoselenosemicarbazone complexes have previously been evaluated for pharmacological uses[25−27] but no metal complexes of bis(selenosemicarbazone) ligands are known, and only one bis(selenosemicarbazone) ligand, **1b**, has been previously reported.[28]

Results

Ligands. The synthetic route (Scheme 1) employed here for the bis(selenosemicarbazone) ligands **1a**−**c** gave higher yields than that previously reported for **1b**[28] but also gave traces of dark precipitate of selenium. This is typical of selenosemicarbazides[29] and was minimized by performing the reaction quickly. Residual selenium was removed by reprecipitating from filtered dimethyl sulfoxide (DMSO) solutions with water, but purification of **1a** and **1b** was compromised by further gradual decomposition in solution. While the sulfur analogues were isolated as white powders, **1a**−**c** were off-white to tan. Both types of ligands were poorly soluble in all common solvents except DMSO and dimethylformamide (DMF). The sulfur ligands dissolved in aqueous sodium hydroxide, but the selenium ligands hydrolyzed under these conditions.

The spectroscopic properties of the ligands confirmed their identity. Electron impact mass spectrometry gave molecular ions for **1a** and **1c** but also significant peaks corresponding to polyselenium ions Se_n^+ ($n = 1-7$). In the case of **1b**, molecular ions were not found. Its identity was confirmed by FAB-MS, which showed molecular ions MH^+ and M^+ but no polyselenium ions.

The ^{13}C and ^1H NMR spectra were similar to those of the sulfur analogues, the main difference being a 4 ppm upfield shift in the C═Se carbon resonances compared to the analogous C═S carbon. The resolution of the terminal hydrogen resonances in the ^1H NMR indicates hindrance of rotation of the C−N bond because of significant double-bond character and intramolecular hydrogen bonding.

The IR spectra of **1a**−**c** were similar to those of the bis(thiosemicarbazones). A peak at 840 cm^{-1} assigned to C═S in the bis(thiosemicarbazone) ligands was shifted to 780 cm^{-1} in **1a**−**c**, consistent with the greater mass of Se.[30,31]

Complexes. While bis(thiosemicarbazone) complexes were prepared in basic aqueous solution, selenium-containing ligands (especially in the case of **1a**, less so in the case of **1c**) partially hydrolyzed under these conditions, and **2a**−**c** were instead prepared in DMSO−methanol mixtures. Nevertheless, for **2a** and **2b**, filtration was still necessary to remove traces of selenium, sacrificing some product. Once formed, the complexes were relatively stable in solution, although attempts to grow crystals over extended periods led to decomposition and appearance of crystals of Se_8. Like sulfur analogues **3a**−**c**, **2a**−**c** were red-brown powders poorly soluble in common solvents except DMSO and DMF.

Mass spectra of **2b** and **2c** (but not **2a**), using a variety of ionization modes, gave molecular ions confirming their identity. IR spectra of **2a**−**c** were similar to those of **3a**−**c**. The peak at 780 cm^{-1} in **1a**−**c** (C═Se stretch) was absent from **2a**−**c**.

Electronic Spectra. Electronic spectra of **2a**−**c** in the range 280−900 nm are shown in Figure 1. The spectra of **2a**−**c** and

(17) Lewis, J. S.; Welch, M. J. *Q. J. Nucl. Med.* **2001**, *45*, 183−188.
(18) Lewis, J. S.; McCarthy, D. W.; McCarthy, T. J.; Fujibayashi, Y.; Welch, M. J. *J. Nucl. Med.* **1999**, *40*, 177−183.
(19) Obata, A.; Yoshimi, E.; Waki, A.; Lewis, J. S.; Oyama, N.; Welch, M. J.; Saji, H.; Yonekura, Y.; Fujibayashi, Y. *Ann. Nucl. Med.* **2001**, *15*, 499−504.
(20) Takahashi, N.; Fujibayashi, Y.; Yonekura, Y.; Welch, M. J.; Waki, A.; Tsuchida, T.; Sadato, N.; Sugimoto, K.; Itoh, H. *Ann. Nucl. Med.* **2000**, *14*, 323−328.
(21) Takahashi, N.; Fujibayashi, Y.; Yonekura, Y.; Welch, M. J.; Waki, A.; Tsuchida, T.; Sadato, N.; Sugimoto, K.; Nakano, A.; Lee, J. D.; Itoh, H. *Ann. Nucl. Med.* **2001**, *15*, 293−296.
(22) Takahashi, N.; Fujibayashi, Y.; Yonekura, Y.; Welch, M. J.; Waki, A.; Tsuchida, T.; Nakamura, S.; Sadato, N.; Sugimoto, K.; Yamamoto, K.; Ishii, Y. *J. Nucl. Med.* **1998**, *39*, 53P.
(23) Maurer, R. I.; Blower, P. J.; Dilworth, J. R.; Reynolds, C. A.; Zheng, Y. F.; Mullen, G. E. D. *J. Med. Chem.* **2002**, *45*, 1420−1431.
(24) Dearling, J. L. J.; Mullen, G. E. D.; Lewis, J. S.; Welch, M. J.; Blower, P. J. *J. Labelled Compd. Radiopharm.* **1999**, *42* (Suppl. 1), S276−S278.
(25) Klayman, D. L.; Scovill, J. P.; Bartosevich, J. F.; Mason, C. J. *Eur. J. Med. Chem.* **1981**, *16*, 317−320.
(26) Garg, B. S.; Kurup, M. R. P.; Jain, S. K.; Bhoon, Y. K. *Transition Met. Chem. (London)* **1988**, *13*, 92−95.
(27) Panell, L. K.; Fales, H. M.; Scovill, J. P.; Klayman, D. L.; West, D. X.; Tate, R. L. *Transition Met. Chem. (London)* **1985**, *10*, 141−147.
(28) Keiko, N. A.; Mamashvili, T. N.; Rassolova, G. V.; Kashik, T. V.; Kalikhman, I. D.; Voronkov, M. G. *Bull. Acad. Sci. USSR, Div. Chem. Sci. (Engl. Transl.)* **1984**, *33*, 561−564.
(29) Goddard, D. R.; Lodam, B. D.; Ajayi, S. O.; Campbell, M. J. *J. Chem. Soc. A* **1969**, 506−512.
(30) Gingras, B. A.; Suprunchuk, R. W.; Bayley, C. H. *Can. J. Chem.* **1965**, *43*, 1650−1655.
(31) Sathyanarayana, D. N.; Volka, K.; Geetharani, K. *Spectrochim. Acta, Part A* **1977**, *33*, 517−522.

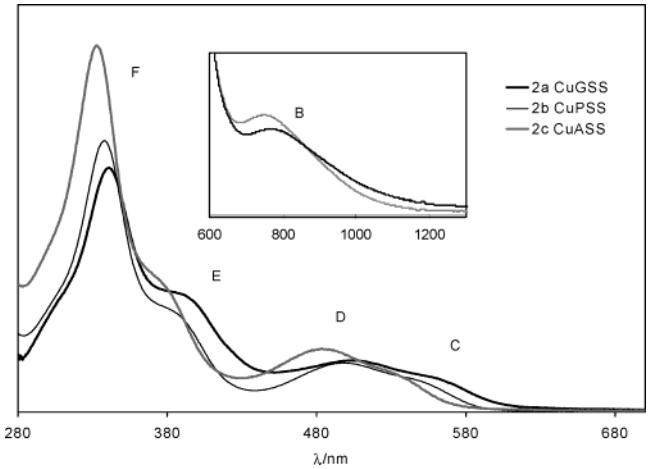

Figure 1. UV−visible spectra of the copper(II) bis(selenocarbazone) complexes **2a**−**c**. Inset is the 600−1300 nm region with absorbance axis expanded by a factor of approximately 100. Assignments of the five main bands labeled B, C, D, E, and F are discussed in the text. Band A, seen in **3a**−**c** (Figure 2), cannot be identified in **2a**−**c** and may be obscured by band B.

3a−**c** are similar in structure. There are six bands, designated A−F. Bands C−F are intense (2000−27 000 mol^{-1}·L·cm^{-1}), while A and B are weak (70−100 mol^{-1}·L·cm^{-1}). In **2a**−**c**, band B is a distinct peak, whereas in **3a**−**c** it appears as a shoulder. No shoulder corresponding to band A of **3a**−**c** is seen in **2a**−**c**, presumably because is it obscured by band B, which is red-shifted compared to its counterpart in **3a**−**c**. No additional features with extinction coefficients greater than 10 mol^{-1}·L·cm^{-1} were detectable between 900 and 2200 nm. Figure 2 shows that in **2a**−**c** the shifts in bands B−F caused by successive methylations closely parallel those in **3a**−**c**: all four peaks are blue-shifted by about 1000 cm^{-1} (500 cm^{-1} per methyl group). Replacing the sulfur atoms in **3a**−**c** with selenium causes a modest red shift in band B (approximately 1300 cm^{-1}), a very slight red shift (about 250 cm^{-1}) in bands C and D, and a large red shift in the higher-energy transitions E and F (about 2000 cm^{-1}). The absorption at 350−380 nm (26 000−28 000 cm^{-1}) in the uncomplexed ligands is blue-shifted by about 600 cm^{-1} per additional methyl group and red-shifted by about 400 cm^{-1} by S/Se substitution.

EPR Spectra. As powders, complexes **2a**−**c** gave poorly resolved spectra with either a single broad line (**2a**, $g = 2.072$; **2b**, $g = 2.068$) or a broad line with a shoulder (**2c**, $g_z = 2.120$, $g_{xy} = 2.033$). These spectra did not change significantly when the temperature was decreased. The powder and frozen solution spectra gave similar g values, indicating no gross structural change between solid and solution. In fluid DMSO/EtOH solution at room temperature, ^{63,65}Cu hyperfine and ^{14}N superhyperfine splitting were resolved in the X-band spectra, which were all very similar to one another and to those of **3a**−**c** (Table 1). This is consistent with the close similarity of the density functional optimized geometry of **2d** with that of its sulfur-containing analogue **3d** (vide infra). The difference in splitting by ^{63}Cu and ^{65}Cu was resolved. Freezing the solutions gave rise to X-band spectra such as that shown in Figure 3 for **2c**. Simulations gave the results shown in Table 1, in which the g and A values are consistent between X-band and Q-band and with the expected mononuclear, d^9 square-planar structure.

Replacement of sulfur by selenium causes minor quantitative changes. These include a 0.007 increase in g_{iso} away from the free-electron value, a 4 G increase in A(Cu), and a 1.4 G decrease in A(N). Methylation of the ligand backbone of **2a** marginally decreases g_{iso} by about 0.001 per methyl group and

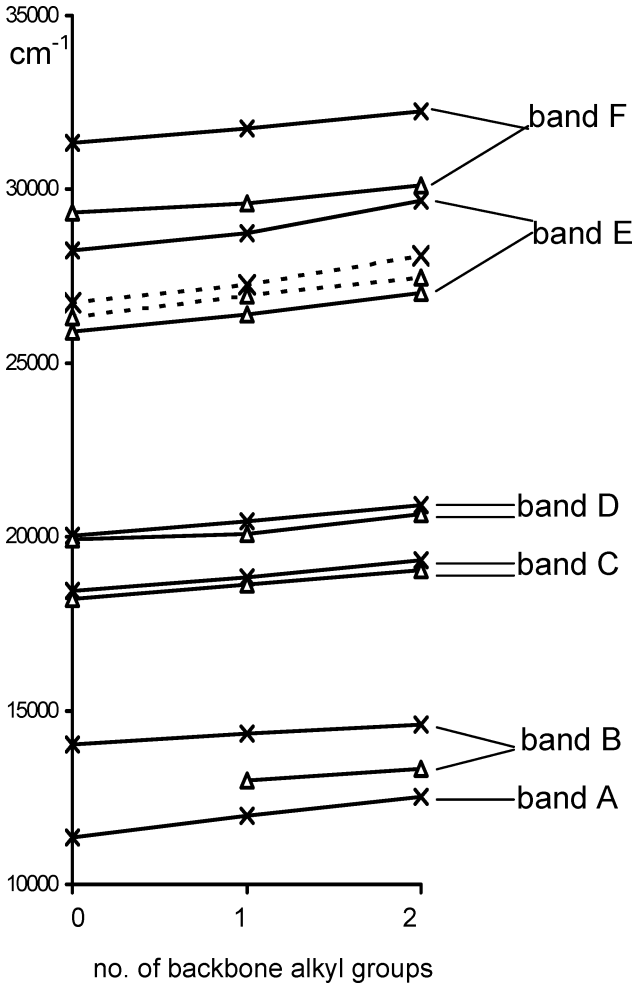

Figure 2. Effect of backbone alkylation and sulfur−selenium substitution on electronic transition energies of the copper bis(thioselenosemicarbazone) complexes and the free ligands. Each line shows the effect of adding methyl groups on one transition (×, sulfur complexes **3a**−**c**; △, selenium complexes **2a**−**c**). The broken line shows the effect on the spectrum of the free ligands. Band A could not be discerned in **2a**−**c**. Band B could not be identified in **2a** because of low solubility and trace impurities.

Table 1. EPR Data for Complexes **2a**−**c** and Sulfur Analogues

	2a	**2b**	**2c**	**3a**–**c**[b]
	Fluid 1:1 DMSO/EtOH			
g_{iso}	2.0695	2.0684	2.0676	2.0609
A(Cu)[a]/G	95.5	95.5	95.5	92.0
	102.2	102.2	102.2	98.3
A(2N)/G	14.0	14.0	14.0	15.4
	Frozen 1:1 DMSO/EtOH			
g_z	2.148	2.142	2.128	2.115
g_x	2.024	2.024	2.024	2.030
g_y	2.037	2.037	2.037	2.030
A_z(Cu)[a]/G	178.5	182.0	189.5	192, 205
A_x(Cu)[a]/G	44.5	44.5	44.5	40, 43
A_y(Cu)[a]/G	45.5	46.5	45.5	
A_z(2N)/G	12.5	12.5	12.5	14.0
A_x(2N)/G	15.5	15.5	15.5	16.5
A_y(2N)/G	15.5	15.5	15.5	

[a] ^{63}Cu and ^{65}Cu, respectively, are listed where they were resolved. [b] Representative of all the sulfur analogues, including **3a**−**c**, from ref 9 in which g and A values were indistinguishable between complexes with different backbone alkylation patterns.

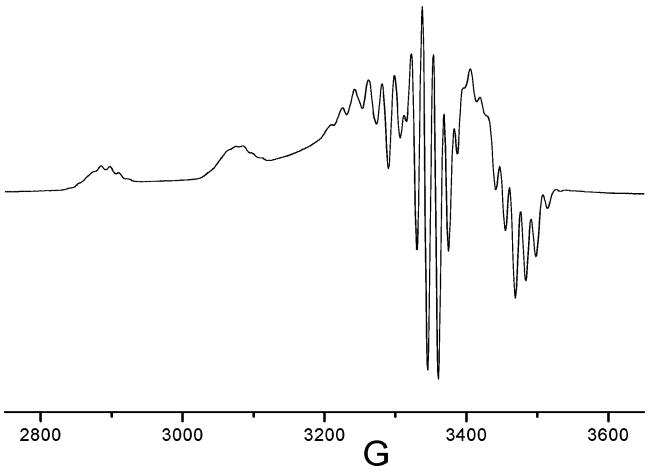

Figure 3. X-band EPR spectrum of CuASS **2c** in frozen DMSO/EtOH solution. For simulated parameters, see Table 1.

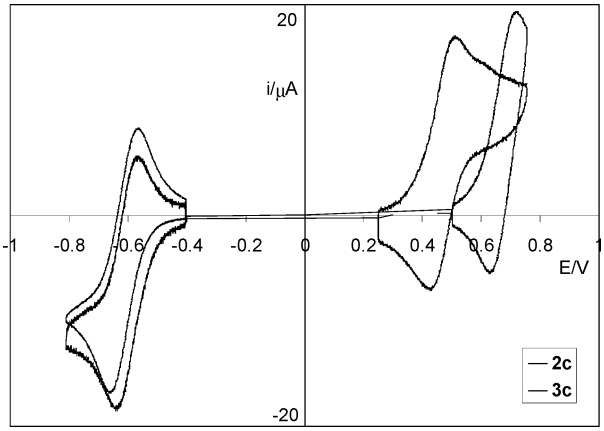

Figure 4. Cyclic voltammograms of **2c** (selenium ligand complex) and **3c** (sulfur ligand complex) showing relative shifts in oxidation potential caused by replacement of sulfur by selenium.

slightly increases A_z(Cu). Coupling to the nitrogen donors is unaffected by alkylation. There is no detectable coupling to the noncoordinated nitrogens as previously suggested[32] but later refuted.[4,33−38]

Electrochemistry. Like the electronic and EPR spectra, the cyclic voltammograms of complexes **2a**−**c** are qualitatively similar to those of their sulfur counterparts. Complexes **2a**−**c** undergo a reversible or partially reversible reduction (**2a**, −0.43 V; **2b**, −0.53 V; **2c**, −0.60 V vs Ag/AgCl) with ΔE_p of ca. 180, 68, and 70 mV, respectively. They also showed a reversible oxidation process (**2a**, 0.53 V; **2b**, 0.49 V; **2c**, 0.47 V, with ΔE_p of 110, 100, and 170 mV respectively). Under the same conditions, ferrocene showed a reversible oxidation at 0.52 V with $\Delta E_p = 68-150$ mV. The oxidation potential for **3a** was close to the limit imposed by the DMSO solvent, making accurate measurement difficult. Figure 4 compares the reduction and oxidation waves of **2c** and **3c**. Figure 5 shows the effects

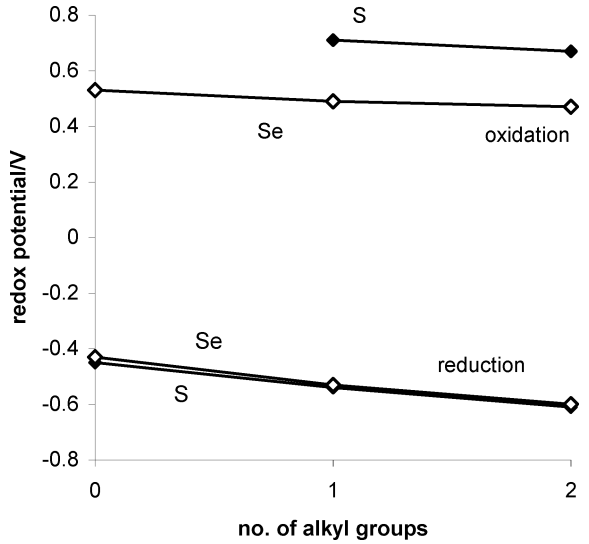

Figure 5. Effect of addition of ligand alkyl groups and replacement of sulfur with selenium on reduction and oxidation potentials of copper bis-(thioselenosemicarbazone) complexes. The top two lines show trends in oxidation potential, and the bottom two lines show trends in reduction potential.

of both backbone methylation and substitution of sulfur by selenium on redox potentials. The Cu(II/I) potentials for the **3a**−**c** measured in this work differ slightly from those previously reported[9] because of differences in experimental conditions, but the trends are the same: for both bis(thiosemicarbazone) and bis(selenosemicarbazone) complexes, each methylation lowers the reduction potential by about 80 mV. Remarkably, replacement of sulfur by selenium affects the reduction potential much less (a positive shift of less than 20 mV) than does methylation. The reversibility of the reduction processes in **2a**−**c** also follows the trend seen in **3a**−**c**:[23] the anodic wave of the Cu(II/I) couple of both **2a** and **3a** (but not **2b**−**c** or **3b**−**c**) is diminished unless the solvent is scrupulously dry, suggesting that the reduced form of **2a** is more susceptible to a proton-dependent reaction than **2b** and **2c**. In contrast to its minimal effect on the reduction process, replacement of sulfur by selenium makes the complex much easier to oxidize (by about 200 mV; Figures 4 and 5). The effect of alkylation on the oxidation potential is relatively modest, compared to both its effect on the reduction potential and the effect of S/Se exchange.

Density Functional Calculations. The optimized geometry for CuATSM **3d** (as manifested in the bond lengths and angles and overall shape) shows excellent agreement with the crystallographically determined geometry of copper bis(thiosemicarbazone) complexes in general[39−43] and showed only marginal distortion from planar C_{2v} symmetry (see Figure 6), although no symmetry was imposed in the calculations. The optimized (hypothetical) selenium analogue **2d** is almost identical to **3d** (Figure 6) except for bonds involving the selenium atoms directly, and for the purposes of labeling the orbitals, nominal C_{2v} symmetry was assumed in both **2d** and **3d**.

(32) Blumberg, W. E.; Peisach, J. *J. Chem. Phys.* **1968**, *49*, 1793−1802.
(33) Getz, D.; Silver, B. L. *J. Chem. Phys.* **1970**, *52*, 6449−6450.
(34) Warren, E. L.; Flowers, J. M.; Hatfield, W. E. *J. Chem. Phys.* **1969**, *51*, 1270.
(35) Warren, E. L.; Horner, S. M.; Hatfield, W. E. *J. Am. Chem. Soc.* **1972**, *94*, 6392−6396.
(36) Antholine, W. E.; Basosi, R.; Hyde, J. S.; Lyman, S.; Petering, D. H. *Inorg. Chem.* **1984**, *23*, 3543−3548.
(37) Campbell, M. J. M. *Coord. Chem. Rev.* **1975**, *15*, 279−319.
(38) Campbell, M. J. M.; Collis, A. J.; Grzeskowiak, R. *Bioinorg. Chem.* **1976**, *6*, 305−311.
(39) Ackerman, L. J.; Fanwick, P. E.; Green, M. A.; John, E.; Running, W. E.; Swearingen, J. K.; Webb, J. W.; West, D. X. *Polyhedron* **1999**, *18*, 2759−2767.
(40) Bushnell, G. W.; Tsang, A. Y. *Can. J. Chem.* **1979**, *57*, 603−607.
(41) John, E.; Fanwick, P. E.; McKenzie, A. T.; Stowell, J. G.; Green, M. A. *Nucl. Med. Biol.* **1989**, *16*, 791−797.
(42) Taylor, M. R.; Gabe, E. J.; Glusker, J. P.; Minkin, J. A.; Patterson, A. L. *J. Am. Chem. Soc.* **1966**, *88*, 1845−1846.
(43) Taylor, M. R.; Glusker, J. P.; Gabe, E. J.; Minkin, J. A. *Bioinorg. Chem.* **1974**, *3*, 189−205.

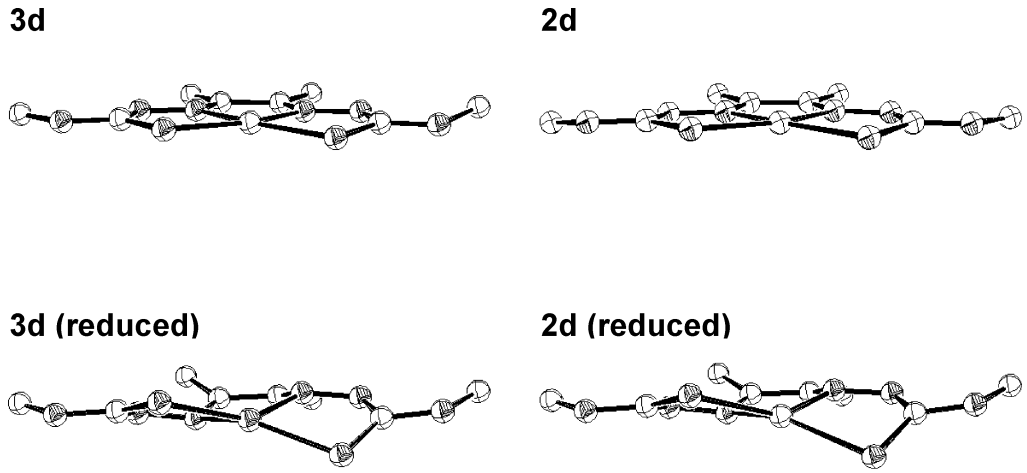

Figure 6. ORTEP representations of minimized geometries of CuATSM **3d** and its selenium analogue **2d** (top) and their one-electron reduced (singlet) forms calculated by density functional methods. The views are selected to show relative deviations from planarity.

The effects of replacing sulfur by selenium were examined by comparing the orbitals and energy levels of complexes **3d** and **2d** (Figures 7and 8). The data for **3d** are taken from calculations using the BLYP functional described previously,[23] which show that the HOMO of CuATSM containing the unpaired electron (α1 in ref 23 and designated $^2b_2\alpha$ in Figures 7 and 8) is a metal−ligand σ-antibonding orbital with $d_{x^2-y^2}$ character, typical of d^9 square-planar complexes. Several filled orbitals below the HOMO ($^1b_1$, $^1b_2$, $^2b_1$, $^1a_2$, $^2a_2$) are ligand-based with minimal contribution from Cu d orbitals (in agreement with semiempirical calculations using the Wolfsberg−Helmholz approximation[35]). With the exception of $^1b_1$ and $^1a_1$, all the orbitals immediately below the HOMO shown in Figure 8 have considerable sulfur p character, and all except the HOMO and $^1b_2$ have ligand π/π^*-character (a_2 or b_1 symmetry). By contrast, the low-lying unoccupied orbitals $^3b_1$ and $^3a_2$, although still having ligand π/π^*-character, have little contribution from sulfur or metal atomic orbitals. The orbitals with principally Cu d character lie much lower ($^2a_1$ and below).

The presence of very low-lying unoccupied orbitals[23] is a key feature of the bis(thiosemicarbazone) complexes. This is preserved in selenium analogue **2d**. There is strong correspondence between the sulfur and selenium analogues in the atomic orbital makeup and ordering of analogous molecular orbitals. In general, the energies of corresponding occupied orbitals were higher for the selenium analogues. The difference is particularly marked (0.32 eV) for the $^2b_1$ orbital, which has almost pure S/Se p character and is raised sufficiently in the Se analogue to alter the energy order, bringing $^2b_1$ above $^1a_2$. By contrast, the unoccupied orbitals, which have relatively little S/Se contribution, are generally slightly lower for the selenium analogues.

To gain insight into the reduction process, the putative singlet ground states of the reduced forms of **3d**[23] and **2d** ($CuATSM^-$ and $CuASSM^-$) were also modeled and optimized, although there is no experimental evidence that these species have more than transient existence. In both cases, the optimized geometry was severely distorted away from planar and toward tetrahedral, with the selenium analogue showing marginally greater distortion (Figure 6). Reduction caused Cu−N bond lengths to increase from ca. 2.05 to 2.10 Å in both complexes and Cu−S and Cu−Se bonds to increase from 2.32 to 2.36 Å and from 2.43 to 2.46 Å, respectively. Despite the distortion, for both sulfur and selenium analogues the character of the original Cu(II) complex orbitals (Figure 8) can still be discerned in the Cu(I) HOMO and LUMO and in HOMO−1 and LUMO+1 (Figure 9), and the orbitals that roughly correspond spatially also follow the same order. This relationship is not obvious outside this range, and C_{2v} symmetry labels have therefore not been used for the Cu(I) orbitals. The distortion removes orthogonality between σ- and π-orbitals. With the HOMO as an example, one can envision a process in which distortion away from planarity allows the original $^3b_1$ orbital to mix into the $^2b_2$ orbital. Thus, the HOMO of both sulfur and selenium Cu(I) complexes has elements of the character of both these two orbitals (Figure 9). Similarly, the LUMO resembles the original $^3b_1$ orbital with some $^2b_2$ orbital character mixed in.

Discussion

The spectroscopic properties of the bis(selenosemicarbazone) complexes **2a**−**c** resemble those of their sulfur analogues (the structures of which are well established[40−45]) so closely that their structural identity as square-planar monomeric Cu(II) complexes cannot be doubted. The analogous S and Se complexes have very similar redox properties, suggesting that **2c** in particular warrants evaluation for hypoxia imaging, since its hypoxia-selective sulfur analogue **3c** has excellent biodistribution properties.[24] Indeed, in vitro evaluation of **2c** in tumor cells confirmed that uptake was strongly hypoxia-selective.[46] Although the instability of the selenosemicarbazone ligands in general is problematic for their radiopharmaceutical application, in the specific case of **2c** the ligand and complex are more stable than the others, and indeed a radiochemically pure complex was easily produced on radiolabeling with ^{64}Cu.[46] The spectroscopic and electrochemical properties of the selenium-containing complexes are of additional interest because of the insight they provide into the electronic structure of the bis(thiosemicarbazone) complexes and the effects of backbone alkylation, which appear to be central to the biological behavior of these versatile imaging agents.[9,23]

(44) Cowley, A. R.; Dilworth, J. R.; Donnelly, P. S.; Labisbal, E.; Sousa, A. *J. Am. Chem. Soc.* **2002**, *124*, 5270−5271.
(45) Castineiras, A.; Bermejo, E.; West, D. X.; El-Sawaf, A. K.; Swearingen, J. K. *Polyhedron* **1998**, *17*, 2751−2757.
(46) McQuade, P.; Lewis, J. S.; Martin, K.; Blower, P. J.; Welch, M. J. Abstract Supplement of the Fifteenth International Symposium on Radiopharmaceutical Chemistry, August 2003, Sydney, Australia. *J. Labelled Compd. Radiopharm.*, in press.

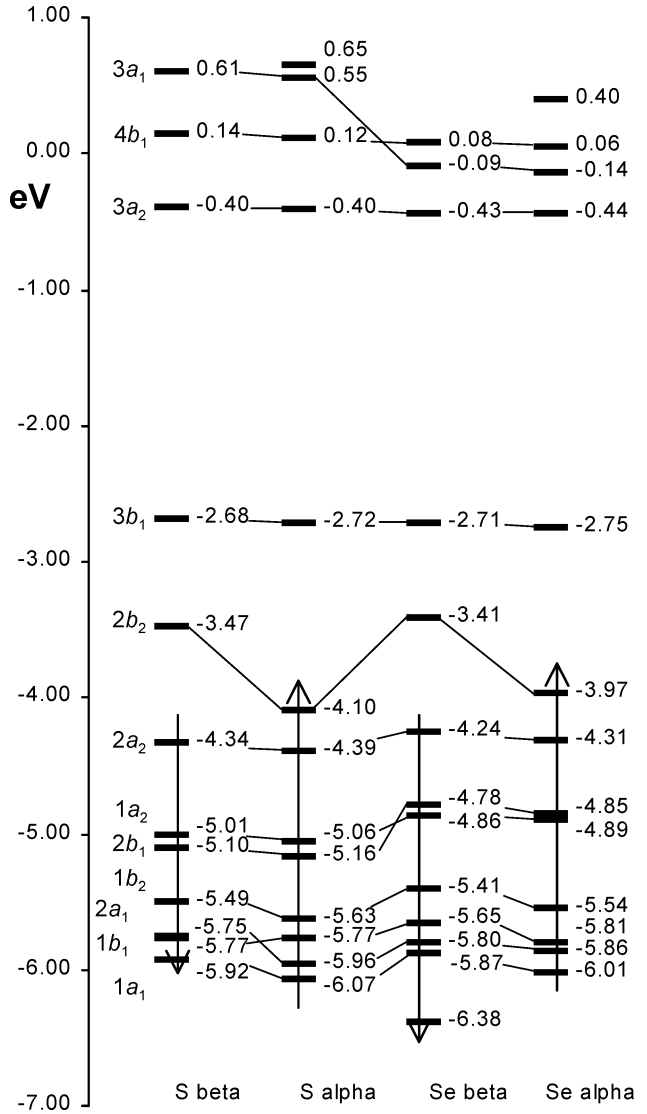

Figure 7. Single-electron molecular orbital energy levels for CuATSM **3d** (sulfur ligand, left) and CuASSM **2d** (selenium ligand, right) showing symmetry labels, with lines to connect orbitals with corresponding symmetry labels. In both cases, the HOMO is the spin-up $^2b_2$ orbital and the LUMO is the spin-down counterpart, and there is a very low-lying unoccupied $^3b_1$ orbital, which can become the LUMO as a result of minor distortions.[23] Symmetry labels assume nominal C_{2v} symmetry, which was not imposed in the optimization.

The main emphasis of the published calculations on CuATSM **3d** and its analogues was on the nature of the electron-accepting orbital in the reduction process.[23] The candidate orbitals found in this earlier work were two very low-lying empty spin orbitals, $^2b_2$ and $^3b_1$ in Figures 7 and 8. One of these ($^2b_2$) was the spin-down partner of the spin-up HOMO, and the other ($^3b_1$) was a ligand-based π-orbital. In the sulfur ligand complexes with no backbone alkyl groups (e.g., **3a**), the energies of these two empty orbitals were very close to each other, and their order was therefore equivocal, depending on subtle changes to geometry and calculation method. In the doubly alkylated complexes (e.g., **3c**), however, the $^3b_1$ was raised more than the metal-centered $^2b_2$, and $^2b_2$ unequivocally became the LUMO. In Figure 7, the $^3b_1$ orbital is indeed above $^2b_2$ in complex **3d**, which has two backbone methyl groups. If the ligand-based $^3b_1$ is the LUMO, reduction would lead to a triplet ground state with the added electron occupying the ligand π-orbital $^3b_1$. If the LUMO is

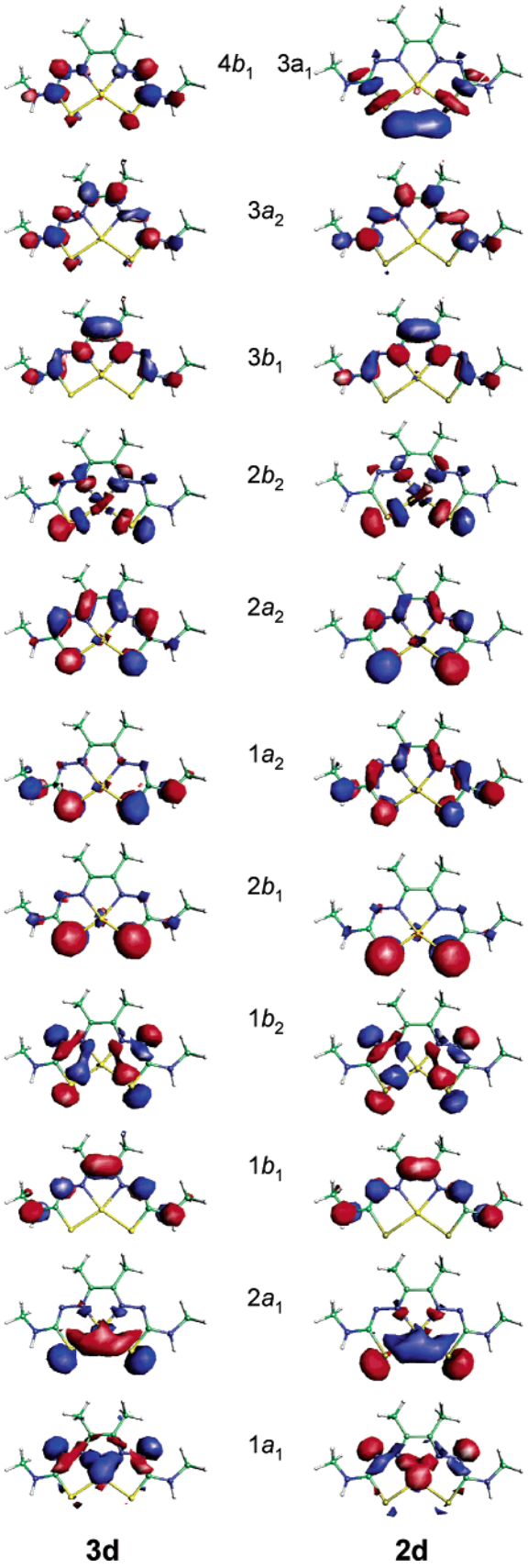

Figure 8. Spatial distribution of calculated one-electron molecular orbitals of CuATSM **3d** (sulfur ligand, left) and CuASSM **2d** (selenium ligand, right). Their energies are shown in Figure 7. Only spin-up (α) orbitals are shown. The HOMO is $^2b_2$ in both cases. The corresponding **3d** and **2d** orbitals are shown side-by-side, except for $^4b_1$ and $^3a_1$.

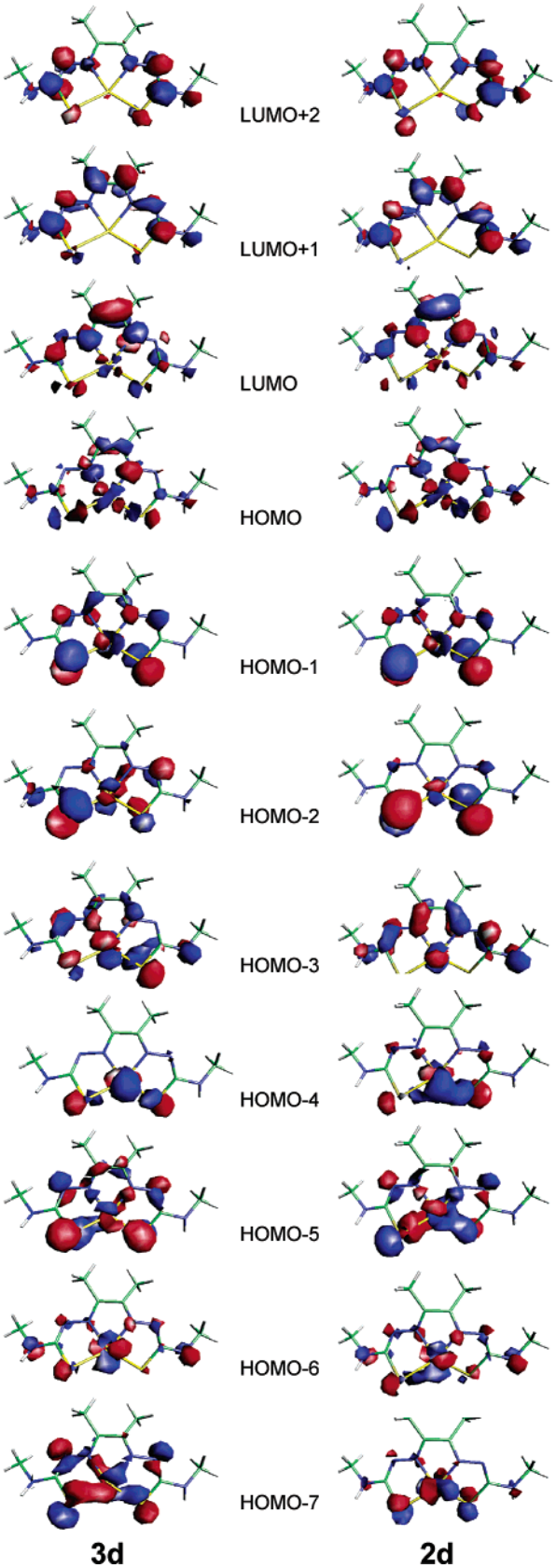

Figure 9. Spatial distribution of calculated two-electron molecular orbitals of $CuATSM^-$ (the one-electron reduced form of **3d**, left) and $CuASSM^-$ (the corresponding reduced form of **2d**, right).

$^2b_2$, reduction would lead to a singlet with electrons paired in the metal-based $^2b_2$. The question of whether copper bis-(thiosemicarbazone) complexes have a triplet reduced state has been raised previously, but attempts to detect it by EPR of electrochemically reduced complexes were inconclusive.[35] If it exists it is highly reactive and short-lived, since reduction of **3d** is known to lead ultimately to a dinuclear singlet Cu(I) species.[44] In the following discussion we compare the selenium- and sulfur-containing complexes to help resolve the uncertainty in the nature of the orbitals involved in the reduction process. A key observation is that the effects on the oxidation potentials of replacing S with Se and of alkylating the ligand backbone are very different to their effects on the reduction potentials. This strongly suggests that the oxidation and reduction involve spatially different orbitals and implicates the low-lying ligand-based $^3b_1$ orbital in the reduction process, as discussed below.

The EPR and electrochemical data identify the $^2b_2$ orbital as the HOMO containing the unpaired electron. We expect the oxidation behavior to reflect the nature of this orbital. The observed oxidation potentials of the complexes are very sensitive to the change from sulfur to selenium (which renders the complexes easier to oxidize by approximately 200 mV; see Figure 5) but relatively insensitive to alkylation (which renders the complexes easier to oxidize by about 30 mV per methyl group). This suggests that the HOMO has significant S/Se character because such an orbital would be raised considerably in energy by replacing sulfur with selenium. The EPR results suggest that it has significant $d_{x^2-y^2}$ character as well (vide infra). Only orbital $^2b_2$ has both of these properties; the density functional calculation suggests that it has $d_{x^2-y^2}$ character and that it is shifted to higher energy by 0.13 eV on replacing sulfur with selenium, in qualitative agreement with the 0.2 V shift in oxidation potential.

The reduction potentials, on the other hand, are barely affected by replacing sulfur with selenium (10 mV shift, cf. 200 mV shift in oxidation potential; Figure 5) but are strongly affected by alkylation, which renders the complexes harder to reduce by about 80 mV per methyl group. Assuming that the reduction potential reflects the properties of the acceptor orbital (i.e., an orbital resembling the LUMO of the Cu(II) complex), these trends are consistent with the acceptor orbital being $^3b_1$ rather than $^2b_2$ because $^3b_1$ is a ligand π-orbital devoid of S/Se character and located largely on the C−C backbone, able to overlap with C−H σ-bonds from the methyl groups. If the LUMO were $^2b_2$ (i.e., if the additional electron became paired with the electron in the $d_{x^2-y^2}$-based orbital), the reduction potentials would have been expected to respond to alkylation and S/Se substitution in the same way as the oxidation potentials.

The electronic structure calculations from the fully optimized geometries identify the LUMO as $^2b_2$, in clear disagreement with the conclusions from the electrochemistry. However, the calculated *shifts* in the energies of the unoccupied orbitals in response to S/Se exchange and alkylation are more in agreement with the electron-accepting orbital being $^3b_1$: the $^2b_2$ orbital is shifted to higher energy by 0.06 eV on replacing sulfur with selenium, whereas the $^3b_1$ is lowered by about 0.03 eV. Thus, if the accepting orbital is $^2b_2$, we should expect that the selenium complex would be harder to reduce by about 60 mV, while if it is $^3b_1$, it would be easier to reduce by about 30 mV. The latter agrees better with the experimental result that the selenium complexes are easier to reduce by about 10−20 mV.

A possible resolution of this conflict can be found in the

electronic structure and geometry calculations on the reduced singlet (d^{10}) species. Since it is known that reduction of **3c** is followed by protonation and rearrangement of metal−ligand bonds to give a dinuclear Cu(I) species,[44] these calculations are only relevant to the initial transient species formed upon reduction and not to the ultimate fate of the reduced complex. However, they do suggest that the initial transient mononuclear reduced species is distorted away from planarity (which may occur as part of a vibrational mode during reduction), mixing $^2b_2$ and $^3b_1$ so that the electron-accepting orbital resembles *both* the $^2b_2$ and the $^3b_1$ (Figure 9). This will lessen the influence of S/Se substitution on the reduction potential and strengthen the influence of alkylation. Thus, although the LUMO in the Cu(II) species is clearly $^2b_2$, the energy of the electron-accepting orbital will be affected by alkylation and by S−Se exchange to some extent as if it were $^3b_1$. The oxidation process, on the other hand, is expected to proceed without distortion to give a square-planar complex isoelectronic with its Ni(II) analogue.[45] The electron donor orbital would thus be pure $^2b_2$, and its energy would respond to alkylation and S−Se exchange accordingly. The mixing of $^2b_2$ and $^3b_1$ caused by distortion may provide a means of interconverting the singlet and any possible triplet-reduced state or, in an alternative view, may provide a mechanism for control of the reduction process through the properties of the $^3b_1$ orbital rather than solely the $^2b_2$. Either argument identifies the presence of the very low-lying empty $^3b_1$ orbital, and its energy and spatial distribution, as the key to controlling the biological behavior of the complexes through structural modifications.

The EPR spectra contribute little to understanding the LUMO, but are consistent with the unpaired electron residing in a HOMO resembling $^2b_2$ in Figures 7 and 8 ($\alpha 1$ in ref 23). The g_{iso} values are greater than the free-electron value, and there is moderately strong hyperfine coupling to the ^{63}Cu and ^{65}Cu nuclear spins. Both the superhyperfine interaction with the coordinated nitrogen atoms and the pattern of the A(N) values ($z < x,y$) are consistent with the participation of the in-plane p orbitals of the coordinated nitrogen atoms in the HOMO $^2b_2$, as shown in Figure 8. The g_{iso} values of the selenium-containing complexes (see Table 1, in which data are in agreement with published results for similar complexes[38,39,45,47]) are higher than those of the sulfur analogues. This is consistent with a significant contribution from sulfur/selenium atomic orbitals to the HOMO since the enhanced spin−orbit coupling contribution from the heavier selenium would shift g_{iso} further from the free-electron value. The observation that methylation alters g_{iso} only marginally, and does not affect the isotropic A(Cu) or A(N) values at all, is consistent with the lack of involvement of the methyl groups in the HOMO. By contrast, replacing sulfur with selenium significantly increases A(Cu) and decreases A(N), suggesting a significant involvement of S/Se orbitals in the HOMO. The ^{63}Cu hyperfine coupling data permits the Cu d orbital population in the HOMO to be estimated as 0.56.[48] Similar treatment of the nitrogen superhyperfine coupling suggests a major contribution (0.08) from each coordinated nitrogen. This implies that the $d_{x^2-y^2}$ component of the HOMO is very much diluted by a large ligand orbital contribution, in agreement with previous estimates of the copper d orbital contribution (0.362 based on g values and between 0.287 and 0.445 based on Wolfsberg−Helmholz semiempirical molecular orbital calculations[35]). The present density functional calculations are in accord with this; they give a Cu d orbital population in the HOMO of 0.26 and a population on each of the coordinating nitrogen atoms of 0.08.

The electronic spectra of the copper bis(thiosemicarbazone) complexes have been reported and variously assigned several times before.[32,35,39,45,47] Because there are many high-energy-filled orbitals and low-energy virtual orbitals, definitive assignments based on absolute orbital energies are unlikely to be reliable, and our commentary is restricted to general trends. The calculations suggest that the observed visible bands A and B may not represent the lowest-energy electronic transitions. Indeed the near-IR spectra show signs of very weak bands (<10 $mol^{-1}\cdot L\cdot cm^{-1}$) between 900 and 2200 nm, but low solubility prevented further analysis in this region. The calculations also predict predominantly red shifts on replacing sulfur with selenium because the calculated energies of the unoccupied orbitals decrease while those of most of the occupied orbitals increase. This is indeed observed, although the shifts in bands C and D are slight. It is interesting to note that in both the sulfur- and selenium-containing complexes, double alkylation causes a strong blue shift of about 1000 cm^{-1} in all observed bands. This corresponds to about 0.12 eV, i.e., of the same order as the shift in reduction potential caused by double alkylation. Replacing sulfur by selenium, however, affects bands C and D much less than bands B, E, and F. This suggests that bands C and D are due to transitions between orbitals with similar S (or Se) contribution ($^1b_2 \rightarrow {}^2b_2$) or between orbitals with negligible S (or Se) contribution ($^1b_1 \rightarrow {}^3b_1$). The large effect of S/Se exchange on bands D and E suggests that these arise from transitions from S/Se-rich orbitals into S/Se-poor orbitals (e.g., $^2a_1 \rightarrow {}^3b_1$ or $^2b_1 \rightarrow {}^3a_2$).

Conclusion

The bis(thiosemicarbazone) and bis(selenosemicarbazone) copper complexes are closely analogous structurally and electronically. From a combination of spectroscopic, electrochemical, and computational results, we conclude that the HOMO in both types of complex is represented by the calculated $^2b_2$ orbital in which the metal d orbital character is highly diluted by ligand σ-character. If we assume that the reversible reduction potential reflects the energy of the acceptor orbital, the added electron should enter an orbital resembling the $^3b_1$ orbital, rather than the spin-down $^2b_2$, and hence, that reduction would lead initially to a triplet state. However, the density functional calculated LUMO is clearly $^2b_2$. This conflict may be resolved by the density functional result that the singlet d^{10} complex is distorted, allowing the $^3b_1$ to mix into the $^2b_2$, thus endowing the accepting orbital with some ligand π-character.

(47) West, D. X.; Ives, J. S.; Bain, G. A.; Liberta, A. E.; Valdes-Martinez, J.; Ebert, K. H.; Hernandez-Ortega, S. *Polyhedron* **1997**, *16*, 1895−1905.

(48) Calculated using

$$A_{||} = \langle A \rangle + P\left[-\frac{4}{7}a^2 + \frac{2}{3}\Delta g_{||} - \frac{5}{42}\Delta g_{\perp}\right]$$

$$A_{\perp} = \langle A \rangle + P\left[\frac{2}{7}a^2 + \frac{1}{3}\Delta g_{||} + \frac{5}{84}\Delta g_{\perp}\right]$$

where $\langle A \rangle = (A_z + A_x + A_y)/3$, P is the electron−nuclear dipolar coupling parameter for ^{63}Cu, and A is the LCAO coefficient of the $d_{x^2-y^2}$ orbital in the HOMO.

Experimental Section

Selenosemicarbazide (98%) was obtained from Acros Organics (Fisher Scientific, Loughborough, United Kingdom), and 2,3-butanedione (97%), glyoxal (40% solution), and pyruvic aldehyde (40% solution) were obtained from Aldrich (Poole, United Kingdom). Copper(II) sulfate pentahydrate and all solvents were obtained from Fisons (United Kingdom). Selenium-containing compounds were shielded from light during synthesis and storage. Elemental analysis was performed by the Analysis Centre, University of Kent. ^{1}H and ^{13}C 270 MHz NMR spectra were obtained with a JEOL GSX270 FT instrument in DMSO-d_6. FAB$^+$ (cesium ion bombardment, 3-nitrobenzyl alcohol matrix) and EI mass spectra were obtained by the EPSRC National Mass Spectrometry Service Centre, University of Wales, Swansea, United Kingdom. Infrared spectra were obtained from Nujol mulls between KBr disks by using an ATI Mattson Genesis FTIR spectrometer. Electronic spectra of samples in DMSO were collected on a Unicam UV 500 spectrophotometer in the UV and visible and on a Cary 5 spectrophotometer in the near IR. EPR spectra were obtained by the EPSRC EPR Spectroscopy Service Centre, University of Manchester, using powders, room-temperature fluid DMSO/ethanol solutions at X-band, or frozen 1:1 DMSO/ethanol glasses at X- and Q-band in the temperature range 100−300 K. Cyclic voltammetry was carried out using an EG&G Instruments Scanning Potentiostat 362, a Condecon 310 controller, and Condecon 320 v3.20R software. A glassy carbon working electrode, a platinum wire auxiliary electrode, and an aqueous Ag/AgCl reference electrode were used in 0.1 M tetrabutylammonium hexafluorophosphate in DMSO dried over 0.4 Å molecular sieves and degassed with dinitrogen.

Ligand Synthesis. Bis(thiosemicarbazone) analogues of **1a**−**c** and their copper complexes **3a**−**c** were prepared as described previously.[9,49] *Glyoxal bis(selenosemicarbazone)* **1a**, *pyruvaldehyde bis(selenosemicarbazone)* **1b**, and *2,3-butanedione bis(selenosemicarbazone)* **1c** were prepared from glyoxal, pyruvaldehyde, and 2,3-butanedione, respectively, by a generic method illustrated here by **1b**. Selenosemicarbazide (0.500 g, 3.62 mmol) was added to 5% aqueous acetic acid (25 mL) and stirred at 60 °C, followed immediately by addition of pyruvic aldehyde (0.61 mL, 7 mmol) over 5 min. The initially pink solution rapidly gave a pale yellow to orange-brown precipitate. The suspension was stirred at room temperature for 24 h. The product was collected by filtration, washed with H_2O (3 × 20 mL) and propan-2-ol (20 mL), and dried in vacuo. It was purified by reprecipitating from DMSO with water. Analysis and spectra were as follows:

1a: yield: 93%. Anal. Calcd for $C_4H_8N_6Se_2$: C, 16.1; H, 2.7; N, 28.2. Found: C, 16.0; H, 2.7; N, 27.2. MS (EI, $^{80}Se_2$ isotope peak) *m*/*z*: 300 (M^+, 100%). ^{1}H NMR: δ = 11.98 (s, 2H, NNH), 8.82 (s, 2H, NHH), 8.45 (s, 2H, NHH), 7.80 (s, 2H, CH). ^{13}C NMR: δ = 174.20 (C═Se), 141.62 (N═CH). IR: 3359 (s), 3235 (s), 3157 (s) (N−H stretch), 1609 (s), 1508 (s) (C═N stretch), 782 (s) C═Se stretch. UV: 380 (35 000), 295 (11 000).

1b: yield: 89%. Anal. Calcd for $C_5H_{10}N_6Se_2$: C, 19.2; H, 3.2; N, 26.9. Found: C, 19.9; H, 3.3; N, 26.0. MS (EI, $^{80}Se_2$ isotope peak): only peaks assignable to Se_n^+ (n = 1−5) were detected. FAB$^+$ *m*/*z*: 315 (M + H$^+$, 100%), 314 (M^+, 30%). ^{1}H NMR: δ = 11.97 (s, 1H, NNH), 10.63 (s, 1H, NNH), 8.88, and 8.81 (2 × s, 1H each, NHH, and NHH), 8.46 (s, 2H, NHH, and NHH), 7.75 (s, 1H, CH), 2.15 (s, 3H, CH_3). ^{13}C NMR: δ = 175.16 (Se═C), 174.56 (Se═C), 148.73 (C−CH_3), 143.58 (C−H) 11.13 (CH_3). IR: 3373 (m), 3240 (w), 3140 (w) (N−H stretch), 1603 (s), 1565 (s) (C═N stretch), 787 (s) (C═Se stretch). UV: 371 (35000), 287 (11000).

1c: yield: 58%. Anal. Calcd for $C_6H_{12}N_6Se_2$: C, 22.1; H, 3.7; N, 25.8. Found: C, 22.0; H, 3.6; N, 24.3. MS (EI, $^{80}Se_2$ isotope peak) *m*/*z*: 328 (100%, M^+); signals corresponding to Se_n (n = 5−7) were also detected. ^{1}H NMR: δ = 10.45 (s, 2H, NNH), 8.89 (s, 2H, NHH), 8.38 (s, 2H, NHH), 2.18 (s, 6H, CH_3). ^{13}C NMR: δ = 175.13 (C═Se), 149.74 (CCH_3), 11.76 (CCH_3). IR: 3381 (s), 3236 (s), 3190 (s), 3145 (s) (N−H stretch), 1595 (s), 1496 (s) (C═N stretch), 776 (s) (C═Se stretch). UV: 364 (35 000), 278 (11 000).

Complex Synthesis. *Copper(II) glyoxal bis(selenosemicarbazone)* (CuGSS, **2a**), *copper(II) pyruvaldehyde bis(selenosemicarbazone)* (CuPSS, **2b**), and *copper(II) diacetyl bis(selenosemicarbazone)* (CuASS, **2c**) were prepared by a generic method illustrated here by **2b**. **1b** (0.150 g, 0.481 mmol) was dissolved in DMSO (2 mL). Copper(II) sulfate pentahydrate (0.120 g, 0.481 mmol) in MeOH (2.5 mL) was added, and the solution was stirred overnight. The resulting deep-red solution was filtered to remove a trace of black solid, and H_2O (20 mL) was added to precipitate the product as a dark red-brown powder which was recovered by filtration, washed with H_2O (3 × 20 mL) and MeOH (20 mL), and dried in vacuo. Analysis and spectra were as follows:

2a: yield: 47%. Anal. Calcd for $C_4H_6CuN_6Se_2$: C, 13.4; H, 1.7; N, 23.4. Found: C, 13.5; H, 1.7; N, 21.3. MS: no Se- or Cu-containing species detected by EI, CI, FAB, or ES. IR: 3384 (w), 3282 (w) (N−H stretch); 1625 (s), 1570 (s) (C═N stretch). UV: 549 (sh), 502 (4000), 386 (sh), 341 (18 000). Measurement of weak bands at wavelengths longer than 600 nm was precluded by low solubility and trace impurities.

2b: yield: 18%. Anal. Calcd for $C_5H_8CuN_6Se_2$: C, 16.1; H, 2.2; N, 22.5. Found: C, 14.7; H, 2.1; N, 20.0. MS (EI, $^{63}Cu^{80}Se_2$ isotope peak) *m*/*z*: 375 (90%, M^+); peaks corresponding to Se_n^+ (n = 2−7) were also detected. IR: 3367 (w), 3275 (w) (N−H stretch), 1618 (s), 1584 (s) (C═N stretch). UV: 770 (70), 537 (sh), 498 (3700), 379 (sh), 338 (20 000).

2c: yield: 65%. Anal. Calcd for $C_6H_{10}CuN_6Se_2$: C, 18.6; H, 2.6; N, 21.7. Found: C, 18.8; H, 2.6; N, 21.1. MS (EI, $^{63}Cu^{80}Se_2$ isotope peak) *m*/*z*: 389 (M^+), peaks corresponding to Se_n^+ (n = 2−6) were also detected. FAB *m*/*z*: 389 (M^+), 390 (M + H$^+$), no Se_n peaks were detected. IR: 3404 (w), 3281 (m), 3132 (w) N−H stretch, 1627 (s), 1589 (s) (C═N stretch). UV: 750 (100), 525 (sh), 484 (5000), 370 (sh), 332 (27 000).

The sulfur analogues **3a**−**c** were prepared as previously described.[9] Additional electronic spectral data were obtained in the present work as follows: **3a**: 880 (sh), 713 (sh), 542 (sh), 499 (10 000), 354 (sh), 319 (28 000); **3b**: 835 (sh), 697 (sh), 531 (sh), 489 (8000), 348 (sh), 315 (14 000); **3c**: 799 (sh), 685 (sh), 517 (sh); 478 (9000); 337 (sh); 310 (33 000).

Computational Methodology. The quantum mechanical calculations were performed on **2d** and **3d** as representative examples by using density functional methods[50] as implemented in the DGAUSS suite of programs through the UNICHEM graphical user interface.[51,52] All complexes were fully optimized without imposing symmetry (therefore, reported symmetry labels should be considered approximate). The calculations employed the nonlocal Becke'88 functional for exchange[53] and the Lee, Yang, and Parr functional for correlation[54] (together denoted as BLYP), with a DZVP (double-ζ plus valence polarization) basis set.[55] The nonreduced copper complexes are formally in the Cu(II) oxidation state (d^9) (i.e., they possess an unpaired electron in the HOMO). Calculations on the doublet were therefore carried out using the spin-unrestricted formalism.[56] Consequently, the degeneracy between the α (spin-up) and β (spin-down) orbitals is lost. For comparison with physical measurements carried out in DMSO, solution-phase calculations were carried out using the Born model with a spherical molecular cavity of 7.73 Å and a dielectric constant of 46.0 to represent

(49) Gingras, B. A.; Suprunchuk, R. W.; Bayley, C. H. *Can. J. Chem.* **1962**, *40*, 1053−1059.

(50) Parr, R. G.; Yang, W. *Density Functional Theory of Atoms and Molecules*; Oxford University Press: New York, 1989.
(51) Andezelm, J.; Wimmer, E. *J. Chem. Phys.* **1992**, *96*, 1280−1303.
(52) Medawar Centre: Oxford, 2000.
(53) Becke, A. D. *Phys. Rev. A: At., Mol., Opt., Phys.* **2001**, *38*, 3098−3100.
(54) Lee, C. T.; Yang, W. T.; Parr, R. G. *Phys. Rev. B* **1988**, *37*, 785−789.
(55) Godbout, N.; Salahub, D. R.; Andzelm, J.; Wimmer, E. *Can. J. Phys.* **1992**, *70*, 560−571.
(56) Pople, J. A.; Nesbet, R. K. *J. Chem. Phys.* **1954**, *22*, 571−578.

DMSO.[57] This did not significantly affect either the ordering of the orbitals or their relative energies, and the results are not shown. Mulliken population analysis[58] was used to determine the contribution of particular atomic orbitals to molecular orbitals. We note that quantum mechanically derived atomic charges are not uniquely defined (different schemes can give different values),[59] and this may lead to discrepancies with experiment. Nevertheless, while Mulliken charges are inferior to potential-derived charges when incorporated into force fields, they are superior for understanding chemical reactivity because the atomic charges, particularly those on buried atoms such as the Cu, are not contaminated with contributions from distant atomic orbitals.[59]

Acknowledgment. We thank the EPSRC Mass Spectrometry and EPR Spectroscopy Service Centers for support and Mieebi M. Wankasi for technical assistance.

Supporting Information Available: Optimized geometry (atomic coordinates) and orbital energies for **2d** and **3d** and their one-electron reduction products (plain text). This material is available free of charge via the Internet at http://pubs.acs.org.

JA035737D

(57) Riddick, J. A.; Bunger, W. B.; Sakland, T. K. *Organic Solvents: Physical Properties and Methods of Purification*; Wiley: New York, 1986.
(58) Mulliken, R. S. *J. Chem. Phys.* **1955**, *23*, 1833−1840.
(59) Winn, P. J.; Ferenczy, G. G.; Reynolds, C. A. *J. Phys. Chem. A* **1997**, *101*, 5437−5445.